10. A. A. Lushnikov and A. G. Sutugin, "Current state of the theory of homogeneous nucleation," Usp. Khim., No. 3 (1976).
11. L. S. Rothman and W. S. Benedict, "Infrared energy levels and intensities of carbon dioxide," Appl. Opt., 17, No. 16 (1978).
12. V. N. Faizulaev, Kinetics of Heterogeneous Processes in Gasdynamic Lasers [in Russian], Doctoral Dissertation, Fiz. Inst. Akad. Nauk SSSR, Moscow (1979).
13. A. A. Vedeneev, A. Yu. Volkov, et al., A Theoretical and Experimental Study of a Gasdynamic Laser with Thermal Pumping Based on a CO_2-Ar (Xe) Mixture with a Lasing Wavelength of 18.4 μm [in Russian], Fiz. Inst. Akad. Nauk SSSR, Preprint No. 120 (1979).

STATIONARY MODE OF EXPANSION OF A VAPOR HEATED BY RADIATION OR A FAST-PARTICLE FLUX

A. V. Dobkin, T. B. Malyavina, and I. V. Nemchinov

UDC 535.2.532.529.5/6

A high-power radiation or fast-particle flux will evaporate the surface of an obstacle and will heat the vapor to high temperatures, the vapor then expanding with high velocity. A high pressure is set up at the obstacle. These phenomena have recently attracted attention in relation to pulsed controlled fusion CF. The energy sources are mainly lasers and electron beams. Considerable progress has been made recently [1-7] in producing high-power ion beams. Flux densities of the order of 1 GW/cm^2 have been attained with pulse lengths of 0.01-1 μsec [7]. Estimates have been made of the parameters needed to attain the conditions of CF using ion beams [7-10]. There is also a discussion [11] on the scope for using a high-power radiation continuum for this purpose, this being emitted by strong shock waves generated for example by shells accelerated by particle beams.

The interaction of radiation and particle fluxes with obstacles is of interest not only in relation to CF but also in simulating the collisions of micrometeorites with obstacles, the acceleration of microscopic objects to very high speeds, research on the optical properties and equations of state for materials under extreme conditions, diagnosis of radiation beams and sources, and many other scientific and engineering purposes. The heating and motion of the vapor in general constitute very complicated nonstationary processes, which sometimes are two-dimensional. It is desirable to have a simple model on the other hand that enables one to elucidate the trends in the major parameters with the source parameters and the target characteristics.

Estimates have been made [12] on the plasma parameters attained on exposing a target to a proton pulse for the case where the vapor has planar geometry. If the irradiation is sufficiently prolonged, the vapor thickness will be greater than the radius of the spot or radius of curvature of the target. The expansion becomes two-dimensional and the vapor density falls more rapidly than in the planar case. The peripheral vapor layers become transparent to the incident particles, which penetrate to deeper layers. The energy is deposited mainly at distances $r > r_0$, where r_0 is the target radius. A quasistationary plasma corona is produced. The evaporation rate in the target is much less than the plasma expansion speed, and the main part near the target is played by heating by absorption, while far away cooling predominates as a result of the expansion, while there is ongoing acceleration and passage through the speed of sound. This picture has been described in [13, 14] for laser radiation, and the parameters of the moving radially symmetrical plasma were derived for the case of all-round heating due to the inverse bremsstrahlung of the photoelectric effect. In [15] a study was made of the parameters of the stationary corona when laser radiation is absorbed in a layer with a concentration close to critical, while the energy is transferred to deeper layers by electron thermal conduction.

Moscow. Translated from Zhurnal Prikladnoi Mekhaniki i Tekhnicheskoi Fiziki, No. 6, pp. 14-22, November-December, 1982. Original article submitted June 4, 1981.

There are also studies of the effects of high-power continua on obstacle heating when the vapor expands in planar geometry [16-18]. A stationary state can also occur [19] in all-round irradiation of a spherical target by nonequilibrium continuum radiation. By analogy with [13, 14, 19] we examined the stationary corona for the case where the bombardment is by ions or radiation fluxes and the energy transfer near the sphere occurs under conditions close to those of radiative thermal conduction.

1. The vapor density at the surface of the target is high when a sufficient radiation flux density is incident on a sphere from vacuum, and the Rosseland average radiation range in the vapor is $l_R < r_0$; the energy flux is then described by

$$q = -K\partial T/\partial r,\ K = (16/3)\sigma T^3 l_R, \tag{1.1}$$

where K is the radiative thermal conductivity, σ is Stefan's constant, and T is temperature. The speed u of the vapor expansion increases away from the sphere, while the vapor density ρ falls more rapidly than as $1/r^2$. The approximation $l_R \sim T^{\alpha}\rho^{-b}$ applies in the region of multiple ionization, where $\alpha \gtrsim 1$ and $b \approx 2$; as T increases and ρ falls, the vapor becomes more transparent and l_R becomes comparable with r. Here the radiative conduction equation no longer applies. The rapid increase in l_R with r means that not far from the point $r = r_T$ where $l_R = r$ one can neglect the radiation absorption. In the transition zone near r_T strictly speaking one should solve the complete transport equations, but as this zone is narrow we link up the region of almost complete transparency to that of opacity by means of an approximate condition of continuity for the source radiation fluxes with temperature T_∞ and the one-way flux in the optically dense zone

$$q = \sigma T^4 - (1/2)\,q = \sigma T_\infty^4. \tag{1.2}$$

The stationary motion and heating of the spherically symmetrical corona are described by

$$\rho u r^2 = \rho_* u_* r_*^2 = M/4\pi,\quad dp + \rho u du = 0, \tag{1.3}$$
$$M(h + u^2/2) + F = M\left(h_* + u_*^2/2\right) + F_*,$$

where p is pressure, h enthalpy, F the total energy flux through the spherical surface of radius r directed towards the surface, and M is the total mass flow rate. The subscript * denotes the parameters at the point where the passage through the speed of sound occurs.

We consider the conditions for phase transition into the subsonic evaporation wave at the surface of the sphere:

$$\rho_w u_w r_w^2 = M/4\pi,\quad p_0 = p_w + \rho_w u_w^2, \tag{1.4}$$
$$M\left(h_w + u_w^2/2\right) + F_w = -MQ_v,\quad h_w = h(T_w, \rho_w),\quad T_w = T_v(p_w).$$

Here T_V is the equilibrium phase-transition temperature, while subscript w relates to the parameters behind the evaporation wave, p_0 is the pressure ahead of the wave (in the unevaporated material), and Q_V is the heat of evaporation. If p_0 is above the critical value in the van der Waals sense we cannot talk of equilibrium between the two phases. However, the energy may be deposited mainly in the fairly low-density gaseous layers, in which case we can introduce the nominal temperature T_V and use Eq. (1.4) to avoid detailed analysis of the region of dense material with its complete equation of state.

The optical and thermodynamic properties of the hot vapor are given as tables (we use the tables of [20-22] for aluminum, carbon, and bismuth). We represent them as

$$pv = N(T, \rho)R'T,\ h = C(T, \rho)R'T = pv\gamma/(\gamma - 1), \tag{1.5}$$
$$l_R = l_R(T, \rho),\ R' = R/A,\ v = 1/\rho,$$

where R is the universal gas constant, A is the atomic weight of the substance, v is specific volume, and γ is the effective adiabatic parameter.

The equation of state was also used in the differential form

$$dp/p = B_\rho(d\rho/\rho) + B_T(dT/T), \tag{1.6}$$
$$B_\rho = 1 + \partial \ln N/\partial \ln \rho,\ B_T = 1 + \partial \ln N/\partial \ln T.$$

From Eqs. (1.3) and (1.6) we get

$$\frac{dg}{2g}\left(B_\rho - \frac{\rho g}{p}\right) = -\left(\frac{qS^{1/2}B_T}{2KT} + B_\rho\right)\frac{dS}{S},\quad g = u^2,\quad S = r^2. \tag{1.7}$$

It follows from Eq. (1.7) that there is a special point at which the following conditions are obeyed:

$$g = u^2 = B_\rho\left(\frac{p}{\rho}\right) = \left.\frac{dp}{d\rho}\right|_{T=\text{const}}; \tag{1.8}$$

$$\frac{TK}{qS^{1/2}} = -\frac{1}{2}\frac{B_T}{B_\rho}. \tag{1.9}$$

From Eq. (1.8) we get that the transition through the speed of sound (here isothermal) requires that the following relation is obeyed in the sonic section:

$$r_*(dT/dr)_* = \lambda T_*, \quad \lambda = 2B_\rho^*/B_T^*. \tag{1.10}$$

We have $\lambda = 2$ for constant values of N, C, and γ.

2. When the vapor is heated by a flux of fast ions, we assume that the irradiation is spherically symmetrical. Particles moving along the radius to the target are retarded, so the energy ε of an individual particle decreases, but the total particle flux remains constant:

$$F/\varepsilon = F_*/\varepsilon_*. \tag{2.1}$$

The electrostatic and electrodynamic effects are neglected, since it is assumed that the ion beam is neutralized (the contribution from the electrons to the overall energy balance can be neglected). The initial beam divergence and the scattering are considered as negligible, i.e., the ion motion is radially symmetrical. It is realistic for such conditions to be approximated for ions [7]. Collisions with free and bound electrons are incorporated in the particle retardation.

The energy lost by a fast ion $(d\varepsilon/dr)_e$ keV/cm by collision with free electrons in a Maxwellized plasma is determined [23, 24] by

$$-(d\varepsilon/dr)_e = k_1\frac{z\rho}{\varepsilon}L\Phi, \quad k_1 = 1.44\cdot 10^8 z_\alpha^2 A_\alpha/A, \tag{2.2}$$

where z_α is the ion charge ($z_\alpha = 1$ for protons), while A_α and A are the atomic weights of the particle and the plasma ions; $z(T, \rho)$ is the degree of ionization of the vapor, which is given by the table; the particle energy ε is expressed in keV, and $\Phi = 1$ when the particle velocity is larger than the electron thermal velocity and $\Phi < 1$ otherwise, when the thermal electrons may give up part of their energy to the fast particle [23, 24], with L the Coulomb logarithm, which incorporates collisions and waves in the plasma [25].

The following relationship is used for the energy lost by fast particles at bound electrons $(d\varepsilon/dr)_i$ in keV/cm:

$$(d\varepsilon/dr)_i = f(\varepsilon)k_2\rho(z_A - z)/z_A, \tag{2.3}$$

where k_2 is a constant for a particular target ($k_2 = 3.7\cdot 10^4$ for aluminum), $f(\varepsilon)$ is the experimental energy-loss curve for the cold unionized material [26], and z_A is the number of electrons in an atom of the material ($z_A = 13$ for aluminum). The factor $(z_A - z)/z_A$ incorporates the fact that the energy loss is proportional to the number of electrons in a plasma ion. This approach agrees with Bethe's formula [27] for high particle energies, where the velocity exceeds the velocity of the electrons in a plasma ion and is in accordance with the Lindhard–Scharff model [28] or Firsov's theory [29] for low ion energies.

We use the system of equations (1.3) and (1.4) for the case of particles, while the equation of state is put as

$$dh/h = A_p dp/p - A_v d\rho/\rho, \ A_v = (B_\rho/B_T)A_T - A_\rho, \tag{2.4}$$
$$A_p = A_T/B_T, \ A_T = 1 + \partial \ln c/\partial \ln T, \ A_\rho = \partial \ln c/\partial \ln \rho.$$

Instead of (1.7) we get

$$\frac{S}{2}\frac{dg}{dS}\left(1 - \frac{\gamma}{\gamma - 1}A_p + A_v\frac{h}{g}\right) = -\left(\frac{S}{M}\frac{dF}{dS} + A_v h\right), \tag{2.5}$$

which has a singular point at which the following conditions are obeyed:

$$1 - \frac{\gamma}{\gamma - 1}A_p + A_v\frac{h}{g} = 0; \tag{2.6}$$

$$\frac{dF}{dS} = -\frac{A_v}{S} hM. \tag{2.7}$$

We introduce the differential adiabatic parameter γ_d from

$$\gamma_d = \frac{p}{\rho}\frac{dp}{d\rho}\Big|_{S=\text{const}} = \frac{\gamma A_v}{1+(A_p-1)\gamma}. \tag{2.8}$$

Conditions (2.6) and (2.7) become

$$g_* = u_*^2 = \gamma_d^* \frac{\gamma-1}{\gamma_*} h_* = \gamma_d^* \frac{p_*}{\rho_*} = c_*^2. \tag{2.9}$$

Therefore, the flow speed is equal to the adiabatic speed of sound at the special point. At this point there is a definite relation between the radius r_* and the differential particle range $l = \varepsilon/(d\varepsilon/dr)$:

$$r_* = \lambda_* l_*, \ \lambda_1 = 2A_v^*/(\eta+\chi), \ l_* = \varepsilon_*/(k_1^* + k_2^*), \tag{2.10}$$
$$\chi = Q_v/h_*, \quad \eta = 1 + (\gamma_* - 1)\gamma_d^*/2\gamma_*.$$

For fixed N, C, and γ we have

$$\lambda_1 = 4(\gamma + 1 + 2Q_v/h_*)^{-1}, \quad \gamma = \gamma_d.$$

We take the given values of the particle energy ε_0 and the total energy flux F_0 at a large distance from the sphere as boundary conditions.

3. We integrate (1.3) with (1.1) for radiation or (2.1)-(2.3) for particles from the singular point subject to conditions (1.8)-(1.10) or (2.8)-(2.10), which involves an expansion in terms of the small parameter. The system and the conditions at the special point may be represented in dimensionless form by referring all the parameters to the values in the sonic section: $\bar{p} = p/p_*$, $\bar{\rho} = \rho/\rho^*$, etc. For convenience we omit the bars over the dimensionless quantities. The system takes the following form for radiative conduction:

$$\frac{1}{2}\frac{(h-g\varphi)}{gh}dg = \left(\frac{FB_T\lambda}{2KTS^{1/2}B_\rho} - 1\right)\frac{dS}{S},$$
$$\psi = \frac{\gamma(\gamma^*-1)}{\gamma_*(\gamma-1)}, \quad \varphi = \psi(B_\rho^*/B_\rho), \quad g = u^2, \quad S = r^2,$$
$$\rho g^{1/2} S = 1, \quad h + (\eta-1)g + \chi = F(\chi+\eta),$$
$$F = 2KS^{3/2}\lambda^{-1}dT/dS, \quad h = \psi p/\rho, \quad \eta = 1 + (\gamma_* - 1)B_\rho^*/2\gamma_*.$$

At the sonic point we have

$$h = p = \rho = u = g = F = S = \varphi = \psi = K = 1. \tag{3.1}$$

For $|S-1| \ll 1$ we put

$$g - 1 = x(S-1), \ T - 1 = (\lambda/2)(S-1). \tag{3.2}$$

The dimensionless radiative thermal conductivity is represented in the power form $K = k^{-\alpha}\rho^{\beta}$ near the special point, while we neglect the changes in φ, ψ, γ, B_ρ, and B_T; the slope of the integral curve is given by the quadratic equation

$$ax^2 + bx + c = 0; \tag{3.3}$$
$$2a = 1 + (A_\rho/2), \ \omega = 1/(\chi+\eta), \tag{3.4}$$
$$b = (\eta-1)\omega + (\beta - (\lambda A_T/2) + A_\rho(1-\omega-\alpha))/2,$$
$$c = -(\lambda+1)/2 + \beta + (\alpha+\omega)(\lambda A_T/2 - A_\rho).$$

The following is the system of dimensionless equations and the expansion at the special point for proton beams:

$$\frac{1}{2}\frac{(h-g\varphi)}{gh}dg = \left[\frac{dF}{dS}\frac{S}{h}\frac{(\eta+\chi)}{A_v} - 1\right]\frac{dS}{S},$$
$$\frac{dF}{dS} = \frac{1}{2S^{1/2}}\frac{r_*}{\varepsilon_*}\left(k_1^*\frac{z\rho L\Phi}{\varepsilon} + k_1^*\rho\left(\frac{z_A^* - z}{z_A^* - 1}\right)f(\varepsilon)\right),$$
$$\psi = \frac{\gamma}{\gamma_*}\frac{(\gamma_*-1)}{(\gamma-1)}, \quad \varphi = \psi(\gamma_d^*/\gamma_d), \quad z_A^* = z_A/z_*, \quad g = u^2, \quad S = r^2,$$

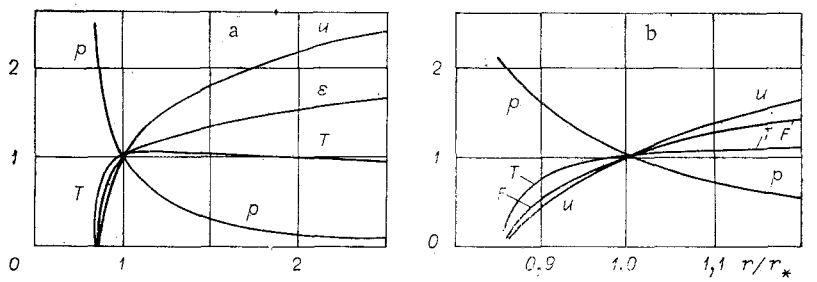

Fig. 1

$$\rho g^{1/2} S = 1, \quad h + (\eta - 1)\, g + \chi = F(\chi + \eta), \quad \varepsilon = F, \quad h = \psi p/\rho,$$

$$k_1^* = k_1 \frac{z_* \rho_*}{\varepsilon_*} L_* \Phi_*, \quad k_2^* = k_2 \rho_* \left(1 - \frac{1}{z_A^*}\right) f(\varepsilon_*), \quad \eta = 1 + (\gamma_* - 1)\, \gamma_d^*/2\gamma_*.$$

At the sonic point we have an addition to Eq. (3.1) that $\varepsilon = z = L = \Phi = 1$; for $|S - 1| \ll 1$ we have instead of Eq. (3.2) that

$$g - 1 = x(S - 1), \quad F - 1 = A(S - 1), \quad A = A_v^*/(\eta + \chi).$$

The dimensionless degree of ionization is represented in the power form $z = h^{-\alpha}\rho^{\beta}$ near the special point, while the changes in φ, ψ, γ_d, γ, A_v, L, Φ can be neglected. To determine the slope of the integral curve we again get Eq. (3.4), where the coefficients are as follows:

$$2a = \eta, \quad b = -(k_\rho + A_v)/2 + k_h(\eta - 1),$$

$$c = 1/2 - k_\rho - k_h A_v + k_\varepsilon A, \quad k_h = \alpha\left[k_{11}^* - k_{22}^*/(z_A^* - 1)\right] + 1,$$

$$k_\rho = 1 + \beta\left[k_{11}^* - k_{22}^*/(z_A^* - 1)\right], \quad k_\varepsilon = k_{22}^* f_1 - k_{11}^*,$$

$$f_1 = [f(\varepsilon_*)]^{-1} \frac{\partial f(\varepsilon)}{\partial \varepsilon}\Big|_{\varepsilon = \varepsilon_*}, \quad k_{11}^* = \frac{k_1^*}{k_1^* + k_2^*}, \quad k_{22}^* = \frac{k_2^*}{k_1^* + k_2^*}.$$

4. We give some results on the plasma parameters for protons of energy 1 MeV (Fig. 1a) and continuum radiation with temperature T_∞ = 24 eV (Fig. 1b) acting on an aluminum sphere of radius r_0 = 1 cm. In the first case, the particle flux density q_0 at the target in the absence of vapor screening will be 22 GW/cm², while in the second it is $q_0 = \sigma T_\infty^4$ = 33 GW/cm². The values of all parameters were referred to their values in the sonic section. About half the beam energy is absorbed in the supersonic region for the protons, and correspondingly ε_* = 0.5 MeV. However, at a distance $r = 2r_*$ the particle energy differs by only 10% from ε_0. The temperature of the supersonic zone differs only slightly from T_* = 20 eV. Near the surface there is a narrow heating zone, and at the surface of the body there is the pressure p_0 = 1.46 GPa, which exceeds p_* by a factor 2.5. The time required for the vapor with speed u_* = 23 km/sec to expand to a distance of the order of the radius of the sphere is about 0.4 μsec. This may be taken as a bound for the time required to establish the stationary state. We use the Rosseland radiation range in the critical section to estimate the thermal-radiation flux q_r^0, which constitutes about 30-50% of the incident energy, and therefore the actual plasma temperature may be appreciably lower than that given. In the radiation case, T_* is also 20 eV, while the pressure at the surface is somwhat higher than that for protons (about 3.9 GPa). Therefore, one expects that the energy loss by radiation with a proton beam in that case, as in [30], will be compensated by the additional evaporation and heating by the radiation from the plasma incident on the target, and the pressure will not be very different from the case where reemission is negligible.

We performed systematic calculations for numerous different cases analogous to that described above, including for conditions where the reemission in the presence of particles is small. Qualitatively speaking, the parameter distribution in each of these cases was analogous to that given in Fig. 1.

In the form shown in Fig. 1b, $l_*/r_* = 0.2$, which shows that the approximation of (1.1) with the condition of (1.2) is permissible. As T_∞ and r_0 increase, the ratio characterizing the degree of opacity decreases and the approximation becomes more accurate. As ρ falls as r increases, while l_R increases very rapidly, the point r_T where $l_R = r_T$ differs only slightly from r_0 and r_* (in the present case $r_* = 1.15$ cm and $r_T = 1.42$ cm). The flux

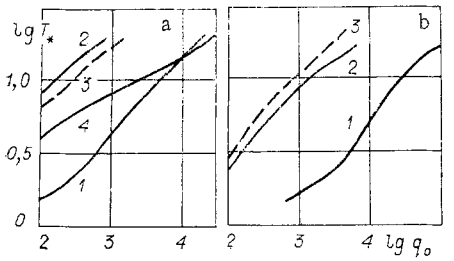

Fig. 2

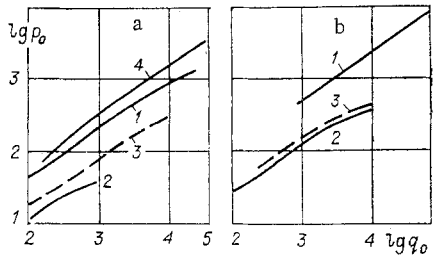

Fig. 3

density of the energy escaping from the optically dense zone can be determined from $q^+ = \sigma T^4 + q/2$ at $r = r_T$; in the present example, the proportion of the energy reemitted backwards is $\xi = q^+/q_0 = 43\%$.

Figure 2 shows the dependence of T_* in eV on q_0 in MW/cm² for protons with $\varepsilon_0 = 1$ MeV (curve 1) and $\varepsilon_0 = 100$ keV (curve 2), as well as for the radiation from a neodymium laser (photon energy $\varepsilon_0 = 1$ eV) in accordance with the calculations of [14] (curve 2), and for radiation in the continuum (curve 4). Figure 2a corresponds to an aluminum sphere of radius $r_0 = 1$ cm, while Fig. 2b corresponds to $r_0 = 0.1$ cm. There is no curve 4 in Fig. 2b because in that case the plasma was transparent and the radiative conduction approximation was incorrect. The plasma heating by protons with $\varepsilon_0 = 100$ keV was close to the heating by the neodymium laser at the same q_0. Heating by the continuum corresponded approximately to heating by protons with $\varepsilon_0 = 1$ MeV. The proton range increases with energy, and the energy of the beam is deposited in a larger mass for the same flux density, which reduces the temperature attained.

Parts a and b of Fig. 2 show the dependence of p_0 in MPa on q_0 in MW/cm² also for $r_0 = 1$ and 0.1 cm correspondingly, while curves 1-4 relate to the same cases as in Fig. 2. As ε_0 increases or r_0 decreases, the target becomes surrounded by a denser plasma and the pressure is higher. The following approximations apply for protons acting on an aluminum sphere at temperatures up to 30 eV:

$$p_0 = 2.3 q_0^{0,6} r_0^{-0,4} \varepsilon_0^{0,75}, \quad T_* = 5.6 q_0^{0,4} r_0^{0,4} \varepsilon_0^{-0,6}. \tag{4.1}$$

For continuum radiation we have

$$p_0 = 0.4 q_0^{0,6} r_0^{-0.3}, \quad T_* = 8 q_0^{0.25} r_0^{0.015} \quad (r_0 \geqslant 1\,\text{cm}), \tag{4.2}$$

and for a laser [14] we have

$$p_0 = 0.07 q_0^{0.67} r_0^{-0.21} \varepsilon_0^{0,42}, \quad T_* = 20 q_0^{0,35} r_0^{0.17} \varepsilon_0^{-0.34}. \tag{4.3}$$

Here the units are as follows: p_0 in GPa, q_0 in GW/cm², r_0 in cm, T_* in eV, for protons the energy ε_0 is in MeV, while for laser radiation the photon energy ε_0 is in eV. Equations (4.1)-(4.3) enable one to compare the heating of the dense plasma by the different sources.

Figure 4 shows the dependence of the energy loss by radiation ξ on q_0 in MW/cm²; here $\xi = q_r^*/q_*$, while q_r^* is the radiation energy flux in the critical section, which is given approximately by

$$q_r^* = \sigma T_*^4 r_*/l_R^* \text{ for } \frac{r^*}{l_R^*} < 1 \text{ or } q_r^* = \sigma T_*^4 \text{ for } \frac{r^*}{l_R^*} > 1.$$

Curves 1 and 2 correspond to $r_0 = 1$ and 0.1 cm with $\varepsilon_0 = 1$ MeV, while curves 3 and 4 correspond to the same r_0 with $\varepsilon_0 = 0.1$ MeV. For $\varepsilon_0 = 0.1$ MeV, the corona is optically thin in

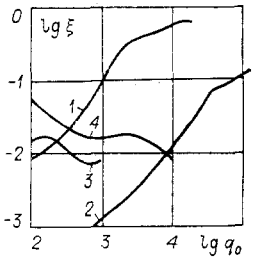

Fig. 4

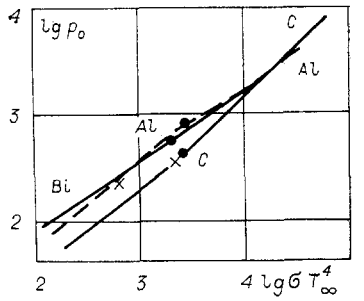

Fig. 5

this temperature range, while it is optically thick for ε_0 = 1 MeV. Correspondingly, the role of reemission is small for low proton energies, while it can become important at high ones, and therefore these estimates need to be refined by direct numerical calculation with detailed allowance for the radiation spectrum, as has been done in [18] for the continuum radiation and in [30] for laser radiation under the conditions of planar geometry on the basis of detailed tables [20-22]. The same applies to continuum radiation for small r_0 and low T_∞.

At the higher temperatures, factors such as the electron thermal conduction may become important. For example, at $q_0 = 5 \cdot 10^4$ GW/cm^2, ε_0 = 10 MeV, and r_0 = 0.4 cm, where $T_* = 100$ eV, the fluxes due to electron thermal conduction constitute about 30% of q_0, and they are of the same order as the radiation loss. With these parameters for the proton beam, the pressure on the target p_0 is about 10^{12} Pa, while the density in the critical section is $\rho_* = 0.1$ g/cm^3.

It is of interest to establish how the target material affects the plasma parameters. Figure 5 gives p_0 in MPa for the surface of a sphere with r_0 = 1 cm in relation to q_0 in MW/cm^2 for targets consisting correspondingly of carbon, aluminum, and bismuth. Crosses denote the points for C and Al for which the optical opacity condition begins to be obeyed, $l_R^*/r_* = 0.3$; for Bi, it is obeyed already at $q_0 = 4$ MW/cm^2. The pressures at the targets of aluminum and bismuth differ only slightly. For C the $p_0(q_0)$ dependence is sharper than that for Al or Bi. The points on the curves denote the q_0 at which $T_* = 10$ eV.

Therefore, sufficiently prolonged irradiation by a high-power proton flux or exposure to continuum radiation can result in quasistationary heating conditions for the dense and hot plasma, which moves at high speed, and the same applies to laser radiation. In some cases the plasma emits intensely. The stationary state may be valuable in plasma diagnosis and in various applications. A similar state can occur when an electron beam is used. A simplified analysis has been given in [31]. However, the neutralization problem may here be more difficult than that for ions, and electrodynamic effects may be more important, as may particle scattering.

LITERATURE CITED

1. S. Humphries, T. J. Lee, and R. N. Sudan, "Generation of intense pulsed ion beams," Appl. Phys. Lett., 25, No. 1 (1974).
2. K. L. Olson, "High-power pulsed ion accelerators for fusion with inertial containment," Fiz. Plazmy, 3, No. 3 (1977).
3. M. A. Greenspan, D. A. Hammer, and R. N. Sudan, "Production of intense focused ion beams in a spherical magnetically insulated diode," J. Appl. Phys., 50, No. 5 (1976).

4. N. V. Filippov and T. I. Filippova, "Subterawatt ion beams at a plasma focus," Pis'ma Zh. Eksp. Teor. Fiz., 29, No. 12 (1979).
5. R. H. Hughes, R. J. Anderson, et al., "Ion beams from laser generated plasmas," J. Appl. Phys., 51, No. 8 (1980).
6. V. A. Gribkov and O. N. Krokhin, "A laser micropinch with combined plasma heating," in: Short Papers on Physics [in Russian], Fiz. Inst. Akad. Nauk SSSR, No. 6, Moscow (1980).
7. S. Humphries Jr., "Intense pulsed ion beams for fusion applications," Nuclear Fusion, 20, No. 12 (1980).
8. F. Wintenberg, "Production of dense thermonuclear plasmas by intense ion beams," Plasma Phys., 17, No. 1 (1975).
9. J. H. Shearer, "Ion beam compression of thermonuclear pellets," Nucl. Fusion, 5, 952 (1975).
10. B. I. Ivanov, A. A. Kalmykov, and D. A. Lavrent'ev, "The scope for initiating thermonuclear reaction by high-current ion beams," Pis'ma Zh. Eksp. Teor. Fiz., 2, No. 3 (1976).
11. F. Wintenberg, "Implosion of black body radiation as a driver for inertial confinement fusion," Atomkernenergie Kerntech., 35, No. 3 (1980).
12. A. V. Dodkin, I. B. Kosarev, and I. V. Nemchinov, "The radiation from the plasma formed by collision of fast particles with a target," Zh. Tekh. Fiz., 49, No. 7 (1979).
13. I. V. Nemchinov, "The stationary state of motion of a radiation-heated vapor in the presence of lateral dispersal," Prikl. Mat. Mekh., 31, No. 2 (1967).
14. T. B. Malyavina and I. V. Nemchinov, "Parameters of a stationary radially symmetrical vapor jet heated by laser radiation," Zh. Prikl. Mekh. Tekh. Fiz., No. 5 (1972).
15. Yu. V. Afanas'ev, E. G. Gamalii, et al., "A stationary model for the corona on a spherical laser target," Zh. Eksp. Teor. Fiz., 71, No. 2(8) (1976).
16. V. M. Krol' and I. V. Nemchinov, "Self-modeling motion in a gas heated by nonequilibrium continuum radiation," Zh. Prikl. Mekh. Tekh. Fiz., No. 5 (1968).
17. V. I. Bergel'son, I. V. Nemchinov, and V. V. Novikova, "The burning of a condensed material under continuum radiation," Fiz. Goreniya Vzryva, 11, No. 5 (1975).
18. V. I. Bergel'son and I. V. Nemchinov, "The heating of an expanding plasma by continuum radiation," Fiz. Plazmy, 7, No. 2 (1981).
19. B. M. Prosvirnina, Stationary Radially Symmetrical Motion of a Vapor Heated by Continuum Radiation [in Russian], VINITI Dep. paper No. 371-79, Moscow (1979).
20. V. P. Buzdin, A. V. Dobkin, and I. B. Kosarev, Radiation Absorption Coefficients and Spectral and Integral Characteristics of the Radiation from an Aluminum Plasma in the Temperature Range $8\text{-}240\cdot10^3$°K at Relative Densities of $3.16\cdot10^{-3}$-100 [in Russian], VINITI Dep. paper No. 370-79, Moscow (1979).
21. G. S. Romanov, K. S. Stepanov, and M. I. Syrkin, "Spectral and average absorption coefficients for a carbon plasma," Zh. Opt. Spektrosk., 47, No. 5 (1979).
22. M. A. El'yashevich, F. N. Borovik, S. I. Kas'kova, G. S. Romanov, K. L. Stepanov, M. I. Syrkin, and V. I. Tolkach, "Thermodynamic functions and absorption coefficients for bismuth and xenon plasmas at temperatures up to 30 eV," in: Abstracts for the Fourth All-Union Conference on Radiating-Gas Dynamics [in Russian], Moscow (1980).
23. B. A. Trubnikov, "Particle collisions in a completely ionized plasma," in: Plasma Theory, M. I. Leontovich, ed., Issue 1 [in Russian], Atomizdat, Moscow (1963).
24. D. V. Sivukhin, "Coulomb collisions in a completely ionized plasma," in: Plasma Theory, M. I. Leontovich, ed., Issue 4 [in Russian], Atomizdat, Moscow (1964).
25. J. Szkarowski, T. Johnston, and M. Baczinski, Plasma Particle Kinetics [Russian translation], Atomizdat, Moscow (1969).
26. Yu. V. Gott, The Interactions of Particles with Matter in Plasma Researches [in Russian], Atomizdat, Moscow (1978).
27. H. Bethe, Quantum Mechanics [Russian translation], Mir, Moscow (1965).
28. J. Lindhard and M. Scharff, "Energy dissipation by ions in the keV region," Phys. Rev., 124, 128 (1961).
29. D. B. Firsov, "A qualitative treatment of the average electron excitation energy in atomic collisions," Zh. Eksp. Teor. Fiz., 36, No. 1 (1959).
30. V. I. Bergel'son and I. V. Nemchinov, "A numerical study of the interaction of a laser with a target under vacuum with allowance for the spectral composition of the radiation emitted by the plasma," Kvantovaya Elektron., 7, No. 11 (1980).
31. R. Gratton, H. Kelly, and V. Pais, "On the properties of the plasma generated by irradiating spherical heavy targets by an electron beam," Plasma Phys., 20, No. 3 (1978).